https://doi.org/10.48048/tis.2023.6965

Blood Flow with Heat Transfer through Different Geometries of Stenotic Arteries

Sumit Kumar[1,*] and Surendra Kumar[2]

[1]*Government College for Women, Gurawara, Rewari, India*
[2]*University Institute Engineering and Technology, Maharshi Dayanad University, Rohtak, India*

([*]Corresponding author's e-mail: sumit96105@gmail.com)

Received: 9 April 2023, Revised: 14 May 2023, Accepted: 21 May 2023, Published: 28 August 2023

Abstract

The current study evaluates blood flow patterns in symmetrical, elliptical, trapezoidal, triangular, cosine-shaped and bell-shaped stenosed arteries with heat transfer. The ordinary differential equations obtained from the transformation applicable to the controlling partial differential equations. The system of ordinary differential equations has been solved using analytical methods of variation of parameters with the help of software. The MATLAB code graphically demonstrates various profiles and analyses the impact of the Prandtl number, magnetic field, Darcy number and Radiation number on velocity, wall shear stress, temperature and volumetric flow rate. The preponderance of blood flow problems is caused by stenosis between z = 1 and z = 2 locations for symmetrical, elliptical, trapezoidal, triangular, cosine-shaped and bell-shaped stenosis. The originality of the present study is the simultaneous influence of varied stenosis geometries on heat transfer. The main observation of blood velocity is that it is also greater for bell-shaped artery walls in the presence of a magnetic field than for trapezoidal artery walls between z = 1 and z = 2 and all other geometries in between. It may help to understand the blood flow in stenosed blood arteries caused by cardiovascular disease.

Keywords: Heat transfer, Symmetrical stenosis artery, Elliptical stenosis artery, Bell-shaped stenosis artery, Oscillatory blood flow, Triangular stenosis artery

Nomenclature

r	Radial direction	k'	Permeability
z	Axial direction	σ	Electrical conductivity
t	Time	B_0	Magnetic field
u	Radial velocity component	β_T	Coefficient of thermal expansion
P	Pressure gradient	T_∞	Reference temperature
ρ	Density	$\bar{g}$	Acceleration by virtue of gravity
μ	Viscosity	K_T	Thermal conductivity
q_r	Radiation absorption coefficient	C_p	Specific heat at constant pressure
$R_1(z)$	Radius of the symmetric stenosed artery	T'	Dimensional temperature
$R_2(z)$	Radius of the trapezoidal stenosed artery	R_0'	Radius of the normal artery
$R_3(z)$	Radius of the triangular stenosed artery	δ_s'	Maximum peak of the stenosis
$R_4(z)$	Radius of the bell-shaped stenosed artery	L_0'	Length of the stenosis
$R_5(z)$	Radius of the symmetric stenosed artery	d'	Location of stenosis
$R_6(z)$	Radius of the cosine-shape stenosed artery	n	Shape parameter
M	Magnetic field	Gr	Groshof number
Pr	Prandtl number	Rd	Radiation parameter
Da	Darcy number	ω	Pulse rate
		θ	Temperature profile

Introduction

To understand blood mechanics, detecting and treating cardiovascular diseases requires studying blood flow through arteries. According to medical surveys, 80 % of people worldwide die from cardiovascular disease, so a treatment or way to stop its spread is urgently needed. The arteries stiffen and create stenosis due to circulatory system malfunction. Stenosis narrows the artery, reducing blood flow. If the stenosis within an arterial blood vessel disrupts the vessel's flow pattern and hemodynamic conditions, and the condition's progressive development within the vessel greatly raises the risk of heart failure. Several studies have looked at the impact of atherosclerosis on blood flow, taking into account many dimensions because of its relevance to human health [1-6]. Three major types of blood vessels exist: Arteries, veinsand capillaries. Except for the pulmonary artery, arteries transport oxygenated blood to the tissues. In the tissues, capillaries facilitate the exchange of oxygen and nutrients. The capillaries also transport deoxygenated blood back to the heart via the veins (with the exception of the pulmonary veins). Kabir *et al*. [7] proposed a study work on numerical simulations of pulsatile transitional blood flow across symmetric stenosed arteries with differing cross-sectional areas. This study demonstrated that the fluid characteristics of the 3 types of arteries differ significantly. Tripathi and Sharma [8] describe a mathematical model with the effect of varying viscosity through arterial stenosis. A model of blood flow through a constricted artery due to heat in the presence of a magnetic field is proposed by Bunonyo *et al*. [9]. Abidin *et al*. [10] explored the problem of unsteady solute dispersion in blood flow using the generalised dispersion model and the Herschel-Bulkley fluid model in an overlapped catheterized stenosed artery.

Many recent studies have focused on mixed convection flows with simultaneous heat and mass transmission and chemical processes due to their numerous applications. The mixing heat and mass transfer problems with chemical reactions have attracted extensive interest [11-14]. Ponalagusamy and Priyadharshini [15] analyzed a computational model of the pulsatile flow of magnetic nano-particles through an artery stenosis in the presence of an external magnetic field and body force. Chitra and Bhaskaran [16] are interested in a mathematical model that describes the unstable blood flow in stenosed arteries with heat transfer. A dispersion model for blood flow in arteries through a porous media with a periodic pressure gradient and the presence of a chemically active solute in the majority of the blood is developed by Roy *et al*. [17]. Manchi and Ponalagusamy [18] discuss the simultaneous study of electro-magneto hydrodynamics and magneto hydrodynamics mechanisms in the incompressible flows of sutterbynano-fluid through a slanted porous tapering artery with multiple stenoses. Mukhopadhyay [19] investigates the pulsating blood flow through a constricted artery while a uniform magnetic field traverses the artery. Hussain *et al*. [20] described a CFD (computational fluid dynamics) based COMSOLmulti-physics (software) simulation model. During the analysis, the composition of the base fluid has been determined to be Newtonian at a high shear rate, and the influence of silver and gold nanoparticles on blood circulation inside artery stenosis has been observed. Khanduri and Sharma [21] determine the impact of electrical conductivity and temperature-dependent variable viscosity on MHD (magneto hydrodynamics) flow. Changdar and De [22] describe the mathematical simulation model of pulsatile Newtonian blood flow with multiple stenoses under periodic body acceleration. Using the finite difference method and the Navier-Stokes equation, they analyzed the presence of multiple stenoses in arteries.

Many studies have focused on buoyancy-induced flows with the combined effect of heat and mass diffusion for more than 3 decades. Due to their significance in several scientific applications, fluid mechanics and heat and mass transport are today regarded as essential disciplines. As temperature changes cause density changes, resulting in free convection, buoyancy forces occur on fluid components [23]. Ponalagusamy and Priyadharshini [24] have presented stress fluid models for pulsatile flow in periodic body acceleration and a magnetic field in porous, tapering arteries. Gandhi *et al*. [25] modeled and analyzed blood movement through a bell-shaped constricted artery adopting magnetic hybrid nanoparticle-based drug delivery with variable viscosity, viscous dissipation and joule heating. Furthermore, Gandhi *et al*. [26] extend their research with unstable MHD hybrid nano-particles through irregular stenosed arteries.

The current science of flow across a narrowed or blocked artery is anticipated to serve as the basis for a variety of biomedical science applications. The cumulative effect of physical attributes may benefit scientists in understanding their findings. To the best of our knowledge, no attempt has yet been made to execute the simultaneous effect of different shapes like as symmetrical, elliptical, trapezoidal, triangular, cosine-shaped and bell-shaped of stenosis arteries with heat transfer. Hence, the preceding investigations prompted us to do this analysis.

The current research initiative is structured as follows: The 1st section is an introduction that outlines the physical quantities utilized in this study and other pertinent research. The geometry of the model and the flow's governing equations are presented in this section, titled materials and methods. The next portion

comprises the transformation of similarity. Moreover, utilizing these similarity transformations, the supplied PDEs are converted to couple ODEs. This section introduces the non-dimensional variables used to create governing equation solutions in the current investigation. The analytical solution describes the mathematical model used to solve different flow profiles. Lastly, there is the findings and graphical analysis part. The results are displayed graphically in MATLAB and then elaborated upon. The graphs are generated to carefully analyze the behavior of the flow parameter.

The present investigation has the following goals and novelty:

1) The effect of magnetic field and Darcy number on a diseased segment of an artery is examined.

2) The effect of heat transfer on diverse stenosis shapes.

3) The simultaneous effect on blood flow of stenosed arteries that is symmetrical, elliptical, trapezoidal, triangular, cosine-shaped and bell-shaped.

Materials and methods

Consider Newtonian, unstable, electrically conducting, incompressible and viscous blood moving past a cylindrical polar coordinate stenosed artery. Bunonyo and Ebiwareme [27], Kumar and Kumar [28] and Hanvey and Bunonyo [29] provided the equations that describe the flow field as:

$$\rho \frac{\partial u'}{\partial t'} = -\frac{\partial P'}{\partial z'} + \frac{\mu}{r'}\frac{\partial}{\partial r'}\left(r'\frac{\partial u'}{\partial r'}\right) - \frac{\mu}{k'}u' - \sigma B_0^2 u' + \rho \beta_T (T' - T_\infty)\bar{g} \tag{1}$$

$$\frac{\partial T'}{\partial t'} = \frac{K_T}{\rho C_p}\left(\frac{\partial^2 T'}{\partial r'^2} + \frac{1}{r'}\frac{\partial T'}{\partial r'}\right) - \frac{q_r}{\rho C_p}(T' - T_\infty) \tag{2}$$

where the symbol $'$ represent the dimensional quantities, $r', z', t', u', P', \rho, \mu, k', \sigma, B_0, \beta_T, T_\infty, \bar{g}, K_T, C_p, q_r$, T' represents the radial coordinate, axial coordinate, time, dimensional velocity, pressure gradient, density, viscosity, permeability, electrical conductivity, magnetic field, coefficient of thermal expansion, temperature, acceleration by virtue of gravity, thermal conductivity, specific heat at constant pressure, radiation absorption coefficient and dimensional temperature profile, respectively.

The mathematical functions of various geometries [4-6,27,28,30] of the stenosed artery's wall are stated as:

$$R_1'(z') = \begin{cases} R_0'\left[A'\left\{L_0'^{(n-1)}(z' - d') - (z' - d')^n\right\}\right] & ;\ d' \le z' \le d' + L_0' \\ R_0' & ;\ otherwise \end{cases} \tag{3}$$

$$R_2'(z') = \begin{cases} R_0' - \frac{4\delta_s'}{R_0'}(z' - d') & ;\ d' \le z' \le d' + \frac{L_0'}{4} \\ R_0' - \frac{\delta_s'}{R_0'}L_0' & ;\ d' + \frac{L_0'}{4} \le z' \le d' + \frac{3L_0'}{4} \\ R_0' - \frac{2\delta_s'}{R_0'}\left[L_0' - 2\left(z' - d' - \frac{L_0'}{2}\right)\right] & ;\ d' + \frac{3L_0'}{4} \le z' \le d' + L_0' \\ R_0' & ;\ otherwise \end{cases} \tag{4}$$

$$R_3'(z') = \begin{cases} R_0' - \frac{2\delta_s'}{R_0'}(z' - d') & ;\ d' \le z' \le d' + \frac{L_0'}{2} \\ R_0' - \frac{2\delta_s'}{R_0'}(L_0' + z' - d') & ;\ d' + \frac{L_0'}{2} \le z' \le d' + L_0' \\ R_0' & ;\ otherwise \end{cases} \tag{5}$$

$$R_4'(z') = \begin{cases} R_0' - \delta_s' e^{-\frac{m^2}{R_0'^2}\left(z' - d' - \frac{L_0'}{2}\right)^2} & ;\ d' \le z' \le d' + L_0' \\ R_0' & ;\ otherwise \end{cases} \tag{6}$$

$$R_5'(z') = \begin{cases} R_0' - \delta_s' \sin\left[\frac{\pi(z' - d')}{L_0'}\right] & ;\ d' \le z' \le d' + L_0' \\ R_0' & ;\ otherwise \end{cases} \tag{7}$$

$$R_6'(z') = \begin{cases} R_0' - \frac{\delta_s'}{2}\left\{1 + cos\left[\frac{2\pi}{R_0'}\left(\frac{L_0'}{2} - z' + d'\right)\right]\right\} ; \ d' \le z' \le d' + \frac{L_0'}{2} \\ R_0' - \frac{\delta_s'}{2}\left\{1 + cos\left[\frac{2\pi}{R_0'}\left(z' - d' - \frac{L_0'}{2}\right)\right]\right\} ; \ d' + \frac{L_0'}{2} \le z' \le d' + L_0' \\ R_0' \qquad\qquad\qquad\qquad\qquad\qquad ; \ otherwise \end{cases} \tag{8}$$

where $R_1'(z')$is the radius of the symmetric stenosed artery, R_0' is the radius of the normal artery in the current model, $R_2'(z')$ is the radius of the trapezoidal stenosed artery, d' is the location of the stenosis, $R_3'(z')$ is the radius of the triangular stenosed artery, δ_s' is the maximum peak of the stenosis such that $\delta_s'/R_0' \ll 1$,$R_4'(z')$ is the radius of the bell-shaped stenosed artery, L_0' is the length of the stenosis, $R_5'(z')$ is the radius of the symmetric stenosed artery, $R_6'(z')$ is the radius of the cosine shape stenosed artery and $A' = \frac{\delta_s'}{R_0' L_0'^n}\left(\frac{n^{(n/(n-1))}}{n-1}\right)$.

The boundary conditions are $\begin{cases} \frac{\partial u'}{\partial r'} = 0, \ \frac{\partial T'}{\partial r'} = 0 \ \ at\ at\ r' = 0 \\ u' = 0, \ T' = T_w\ at\ r' = R_l'(z')\ where\ l = 1,2,3,4,5,6 \end{cases}$

The governing flow equations are written using the following non-dimensional variables in dimensionless form.

$r = \frac{r'}{R_0'}$, $\theta = \frac{T'-T_0}{T_w-T_\infty}$, $u = \frac{u'R_0'}{\nu}$, $z = \frac{z'}{R_0'}$, $t = \frac{t'\nu}{R_0'^2}$, $P = \frac{R_0'^2 P'}{\mu\nu}$, $P_r = \frac{\mu C_p}{K_T}$, $G_r = \frac{\bar{g}\beta_T R_0'^3 (T_w - T_\infty)}{\nu^2}$, $D_a = \frac{k'}{R_0'^2}$,$M^2 = \frac{B_0^2 R_0'^2 \sigma}{\mu}$, $R_d = \frac{q_T R_0'^2}{\mu\, C_p}$

Dimensionless flow equations are:

$\frac{\partial u}{\partial t} = -\frac{\partial P}{\partial z} + \frac{1}{r}\frac{\partial}{\partial r}\left(r\frac{\partial u}{\partial r}\right) - \frac{1}{Da}u - M^2 u + G_r\theta$and $P_r\frac{\partial \theta}{\partial t} = \frac{\partial^2\theta}{\partial r^2} + \frac{1}{r}\frac{\partial\theta}{\partial r} - R_d P_r\theta$

It is considered that the flow is unsteady and pulsating. Thus, the solution is as follows:

$u = u_0 e^{i\omega t}$, $\theta = \theta_0 e^{i\omega t}$, $-\frac{\partial P}{\partial z} = P_0 e^{i\omega t}$

where ω is the angular frequency of oscillations, P_0 is the constant pressure.

After employing the dimensionless transformation variable and condition for pulsatile blood flow, the following is obtained:

$\frac{\partial^2 u_0}{\partial r^2} + \frac{1}{r}\frac{\partial u_0}{\partial r} - \left(\frac{1}{Da} + M^2 + i\omega\right)u_0 = -P_0 - G_r\theta_0$ and $\frac{\partial^2\theta_0}{\partial r^2} + \frac{1}{r}\frac{\partial\theta_0}{\partial r} - (R_d + i\omega)P_r\theta_0 = 0.$

Final solutions after employing boundary conditions determined by the variation of parameter method are given:

$\theta(r,t) = \frac{I_0(\eta\, r)}{I_0(\eta\, R_l)}$ and $u(r,t) = \left[-\frac{P_0 I_0(\varphi\, r)}{I_0(\varphi\, R_l)\varphi^2} - \frac{G_r e^{-i\omega t} I_0(\varphi\, r)}{I_0(\varphi\, R_l)(\varphi^2 - \eta^2)} + \frac{P_0}{\varphi^2} + \frac{G_r e^{-i\omega t} I_0(\eta\, r)}{I_0(\eta\, R_l)(\varphi^2 - \eta^2)}\right] e^{i\omega t}$

where $\eta^2 = (R_d + i\omega)P_r$ and $\varphi^2 = \frac{1}{Da} + M^2 + i\omega$.
The volumetric flow rate (Q) and wall shear stress (τ_w) are defined as:

$Q = 2\pi \int_0^{R_l} r\, u(r,z,t)\, dr$, $\tau_w = \left(-\frac{\partial u}{\partial r}\right)_{r=R_l}$

and obtained volumetric flow rate (Q) and wall shear stress (τ_w) from velocity profile as:

$$Q = 2\,\pi\left[-\frac{P_0 R_l I_1(\varphi\, R_l)}{I_0(\varphi\, R_l)\varphi^3} - \frac{G_r e^{-i\omega t} R_l I_1(\varphi\, R_l)}{I_0(\varphi\, R_l)(\varphi^2-\eta^2)\,\varphi} + \frac{P_0 R_l^2}{2\,\varphi^2} + \frac{R_l G_r e^{-i\omega t} I_0(\eta\, R_l)}{I_0(\eta\, R_l)\,\eta\,(\varphi^2-\eta^2)}\right] e^{i\omega t},$$

$$\tau_w = \left[\frac{P_0 I_1(\varphi\, R_l)}{I_0(\varphi\, R_l)\,\varphi} + \frac{G_r e^{-i\omega t}\,\varphi\, I_1(\varphi\, R_l)}{I_0(\varphi\, R_l)(\varphi^2-\eta^2)} - \frac{G_r e^{-i\omega t}\eta\; I_1(\eta\, R_l)}{I_0(\eta\, R_l)(\varphi^2-\eta^2)}\right] e^{i\omega t}.$$

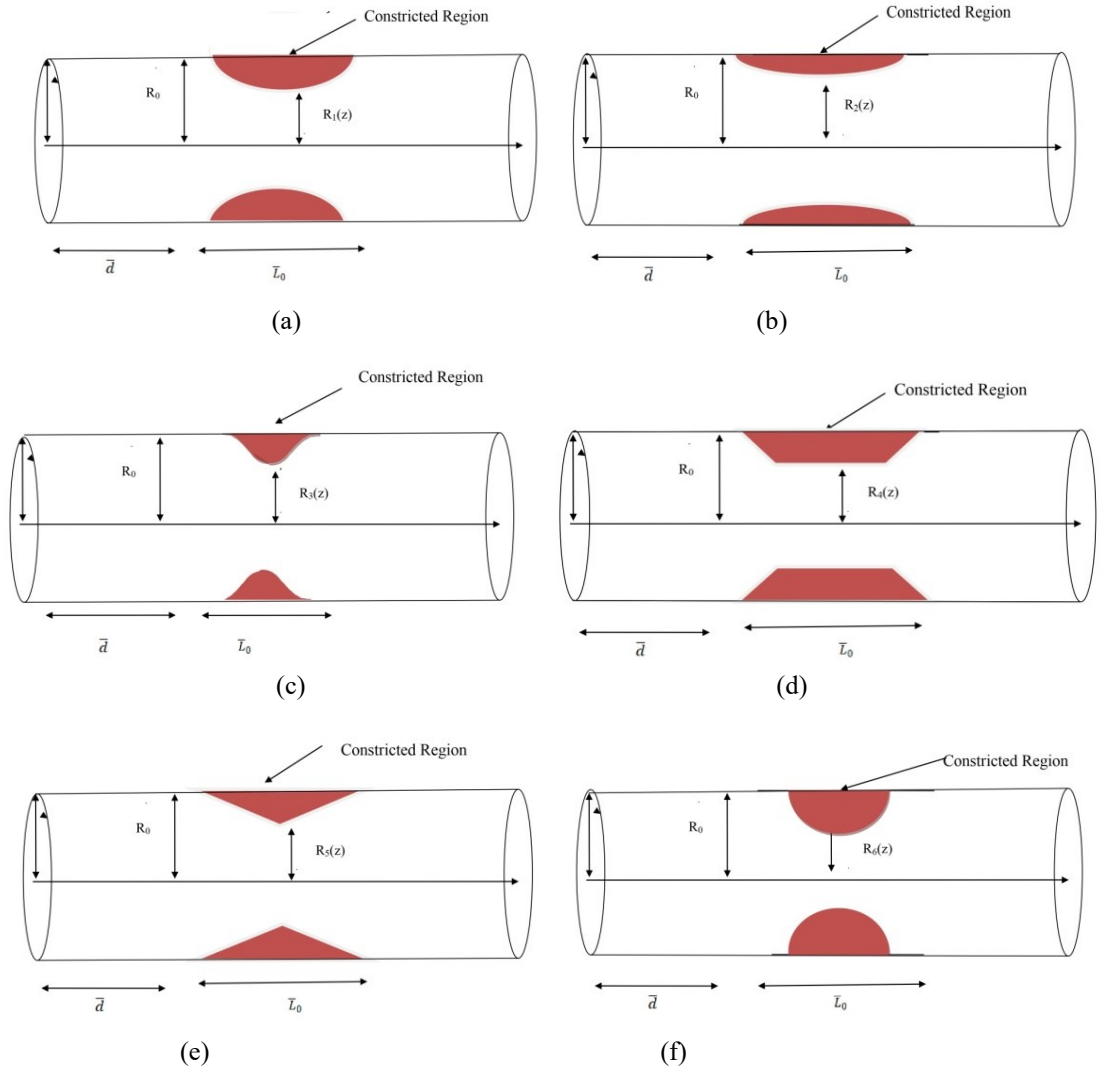

Figure 1 Geometry of (a) symmetric, (b) elliptical, (c) bell-shaped, (d) trapezoidal, (e) triangular and (f) cosine-shaped constricted artery.

Results and discussion

This mathematical study seeks to determine how stenosis influences blood flow through a symmetric, bell-shaped, cosine-shaped, elliptical, trapezoidal and triangular artery. The influence of emergent properties such as Prandtl number (Pr) and radiation (Rd) on blood temperature profiles is studied. There is also a comparison of these profiles for various types of stenotic. Using the variation of parameters method, dimensionless governing equations have been simplified. The velocity, temperature, wall shear stress and volumetric flow rate profiles are computed using MATLAB algorithms. Figures are used to study the flow patterns of many physical elements. The values that will be used by default for this analysis such as $Rd = 2, \mathrm{Pr} = 21, w = 0.5, M = 2, z = 1-2, Gr = 15, P_0 = 10, d = 1, t = 0.2, Da = 0.07, \delta_s = 0.2\,, n = 2, m = 5$[4,6,8,9,16,25-31]. The computational work has been completed by applying the parameter default values as shown above.

Figure 2 illustrates the variation in velocity profiles with respect to radial distance for (a) symmetric, (b) elliptical, (c) bell-shaped, (d) trapezoidal, (e) triangular and (f) cosine-shaped stenosis simultaneously at $z = 1$ and $z = 1.2$ locations. Due to the presence of hemoglobin in RBCs, which contains iron oxide particles and is capable of binding oxygen molecules, the blood is greatly impacted by the magnetic field. The presence of oxygen has a substantial effect on the molecular structure of hemoglobin. Using the magnetic characteristics of blood as inspiration, we numerically characterized the impact of the magnetic field on single-phase blood flow in **Figure 2**. In this study, magnetic field acting in the flow's normal direction generates a Lorentz force perpendicular to the flow's direction, resulting in a decrease in flow velocity. It has also been discovered that under a magnetic field, blood velocity is greater for bell-shaped artery walls than for trapezoidal artery walls between $z = 1$ and $z = 2$ and all other shapes in between. **Figure 2** indicates decisively that as the magnetic field ($M = 1, 2, 3$) strength increases, the Lorentz force becomes more prominent in the flow, resulting in a smaller velocity differential between bell-shaped artery walls and trapezoidal artery walls.

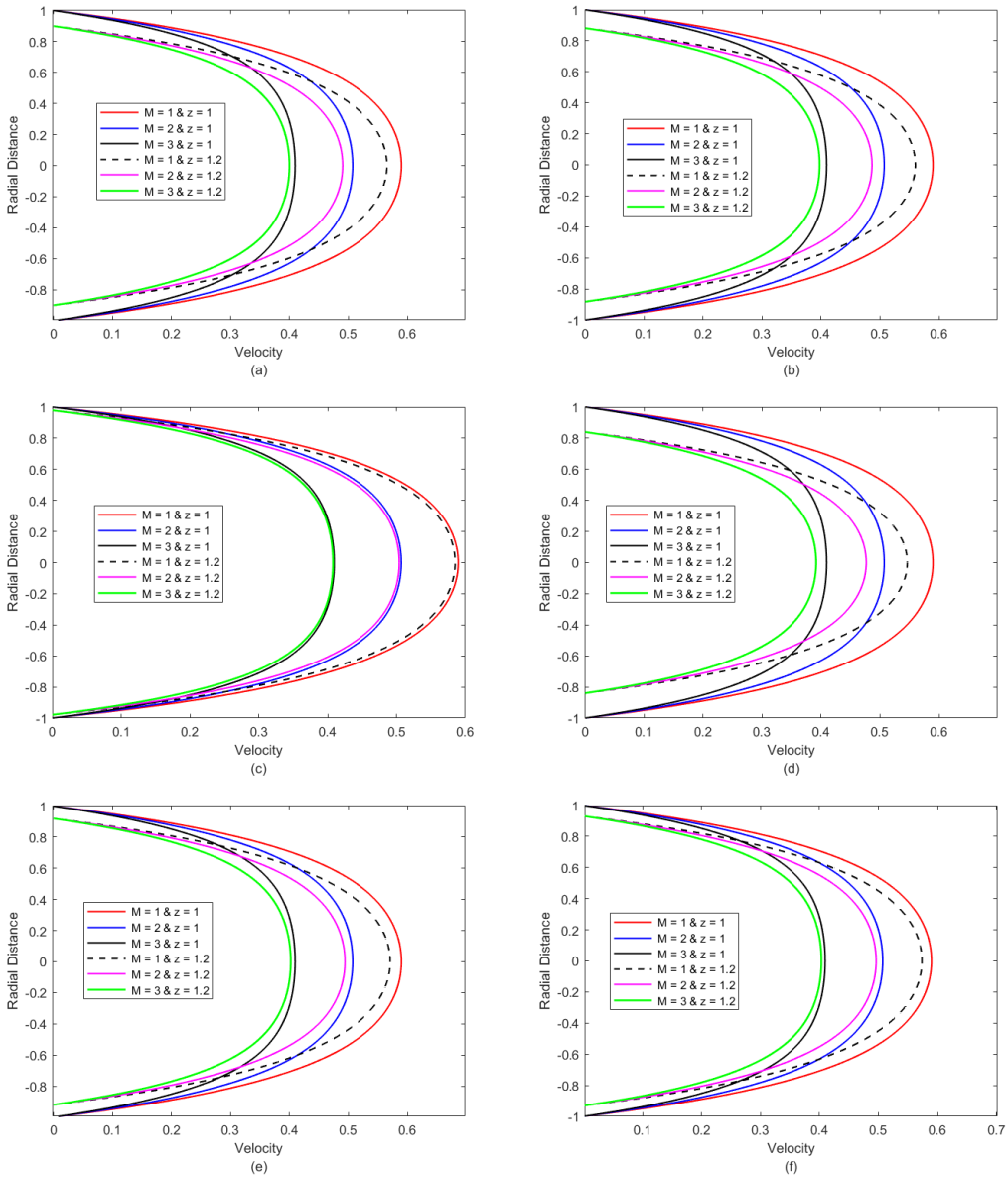

Figure 2 Variations in the velocity profiles of (a) symmetric, (b) elliptical, (c) bell-shaped, (d) trapezoidal, (e) triangular and (f) cosine shapes stenosis artery with $M = 1, 2$ and 3 for various locations of stenotic region $z = 1$ and 1.2.

Figure 3 depicts the variation in velocity profiles as a function of radial distance for (a) symmetric, (b) elliptical, (c) bell-shaped, (d) trapezoidal, (e) triangular and (f) cosine-shaped stenosis simultaneously at $z = 1$ and $z = 1.2$ locations and some specific values of $Da = 0.05, 0.07, 0.09$. If Da increases, the velocity profile improves, showing that the medium's permeability delivers less resistance to the flow, resulting in a rise in velocity. Fundamentally, the Darcy number is connected to the permeability of a porous surface. As the Darcy number grows, the matrix resistance given by solid fibers in porous media decreases, resulting in an increase in the velocity profile of blood flow. Under a Darcy number, blood velocity is greater for bell-shaped artery walls between $z = 1$ and $z = 1.2$ than for all other forms, including symmetrical, elliptical, trapezoidal, triangle and cosine-shaped artery walls. While the blood velocity of trapezoidal-shaped arteries is lower than that of any other shapes.

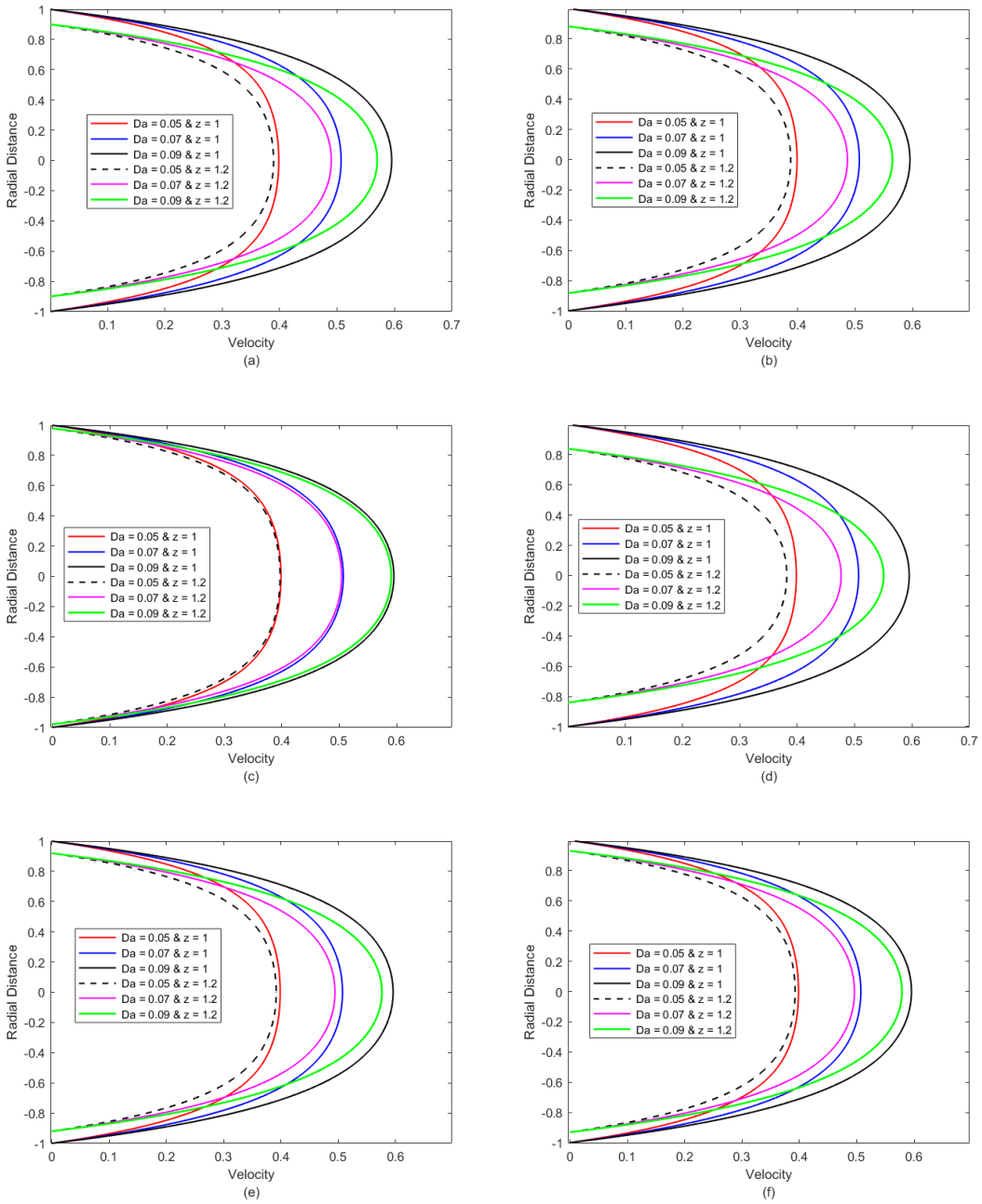

Figure 3 Variations in the velocity profiles of (a) symmetric, (b) elliptical, (c) bell-shaped, (d) trapezoidal, (e) triangular and (f) cosine shapes stenosis artery with $Da = 0.05,\ 0.07$ and 0.09 for various locations of stenotic region $z = 1$ and 1.2.

Figure 4demonstrate the variation in velocity profiles as a function of radial distance for (a) symmetric, (b) elliptical, (c) bell-shaped, (d) trapezoidal, (e) triangular and (f) cosine-shaped stenosis simultaneously at $z = 1$ and $z = 1.2$ locations and some particular values of $P_0 = 7, 10, 13$. The velocity profile improves as the pressure gradient grows because the flow encounters less resistance. Fundamentally, the pressure gradient of blood on blood artery walls generates blood flow pressure. Since pressure measures the force of blood against artery walls, blood flows from high-pressure to low-pressure regions. Blood velocity is greatest in trapezoidal-shaped artery walls between $z = 1$ and $z = 1.2$ under a pressure gradient. Blood velocity is lowest in bell-shaped arteries wall. Bell-shaped arteries have the lowest blood velocity.

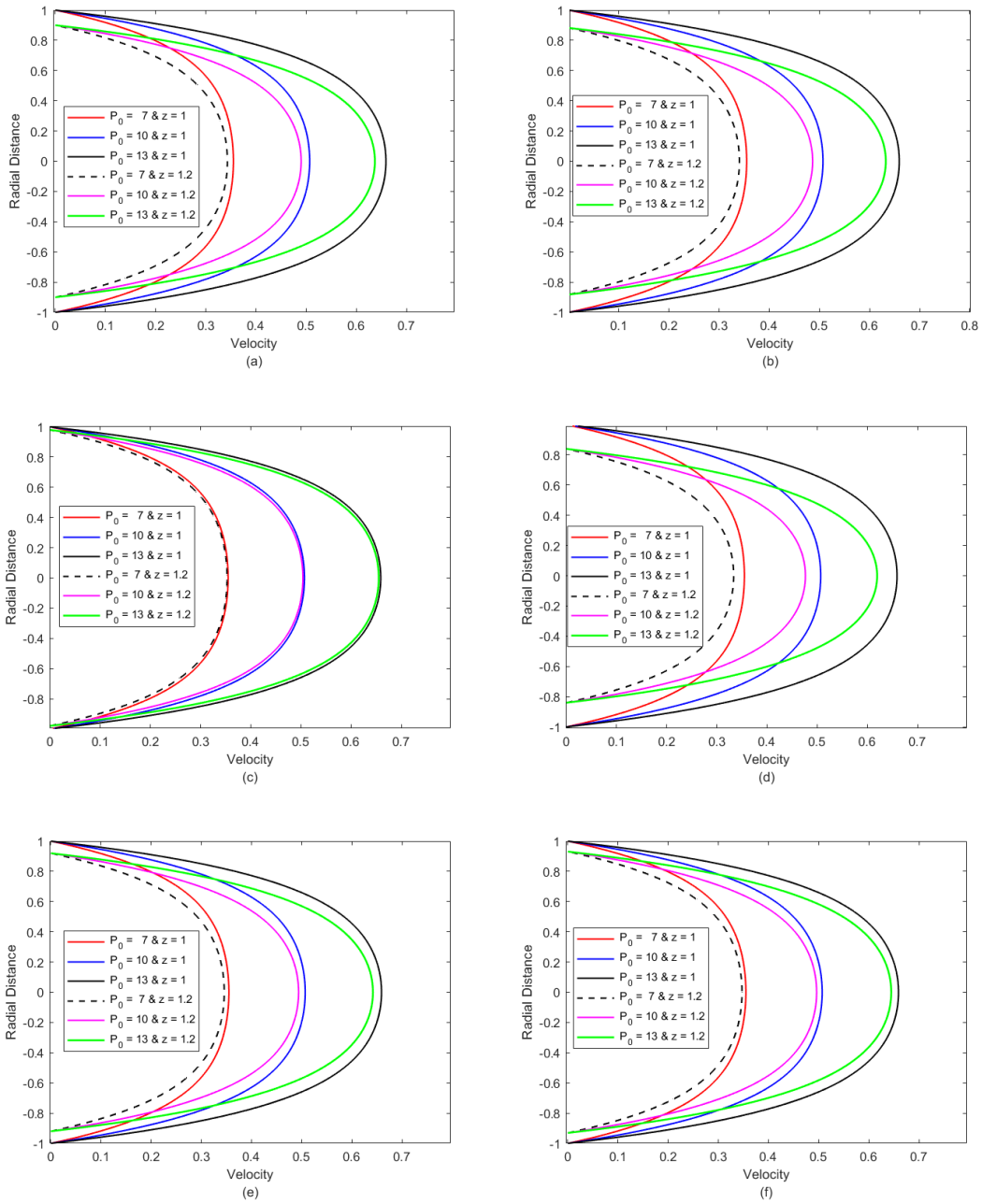

Figure 4 Variations in the velocity profiles of (a) symmetric, (b) elliptical, (c) bell-shaped, (d) trapezoidal, (e) triangular and (f) cosine shapes stenosis artery with $P_0 = 7,\ 10$ and 13 for various locations of stenotic region $z = 1$ and 1.2.

Figure 5 depicts the temperature profile of blood for various geometries and varied values of the Radiation parameter at 2 locations $z = 1$ and $z = 2$. As shown visually, when the radiation parameter($Rd = 1, 2, 3$) increases then the blood temperature decrease. This occurs because plasma is a suspension of erythrocytes, leukocytes and platelets in a fluid. If the stenosis is located at $z = 1.2$, the depth of stenosis for all varieties of stenosis, including symmetric, elliptical, bell-shaped, trapezoidal, triangular and cosine-shaped, differs, whereas at $z = 1$, the radial distance is the same in all circumstances. The graph also reveals that the temperature rises as one move from the artery's center line to the arterial wall.

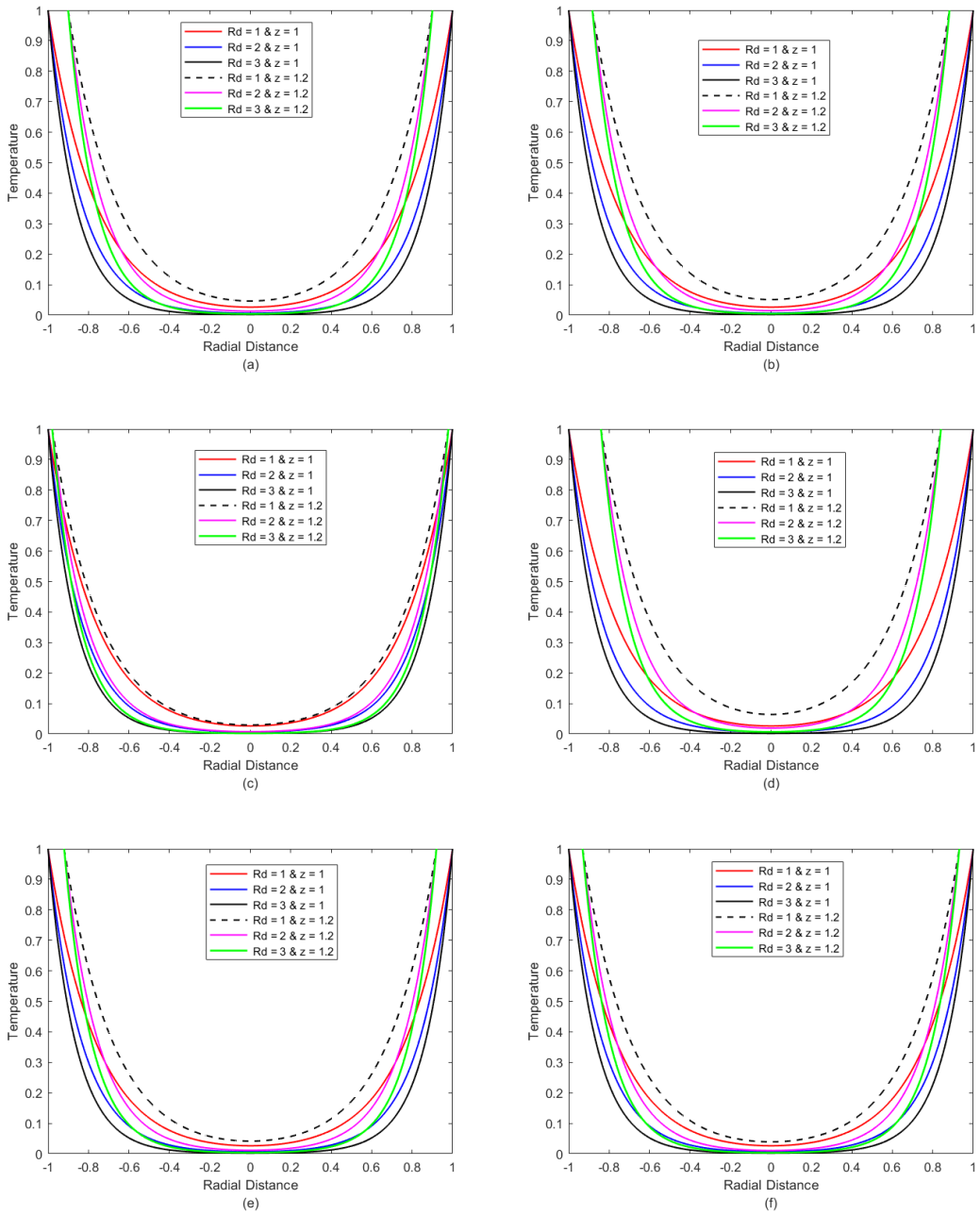

Figure 5 Variations in the temperature profiles of (a) symmetric, (b) elliptical, (c) bell-shaped, (d) trapezoidal, (e) triangular and (f) cosine shapes stenosis artery with $Rd = 1,\ 2$ and 3 for various locations of stenotic region $z = 1$ and 1.2.

Figure 6 depicts the effect of Prandt number on temperature at 2 sites, $z = 1$ and $z = 1.2$, for each of 6 distinct geometries. The Prandtl number is the ratio between momentum and thermal diffusivity. Prandtl number is inversely proportional to the rate of heat transfer from the artery wall to the fluid (blood). As the Prandtl number grows, thermal diffusion decreases, resulting in a temperature drop. If the stenosis is located at $z = 1.2$, the depth of stenosis for all varieties of stenosis, including symmetric, elliptical, bell-shaped, trapezoidal, triangular and cosine-shaped, differs, whereas at $z = 1$, the radial distance is the same in all circumstances. The graph also reveals that the temperature rises as one move from the artery's center line to the arterial wall.

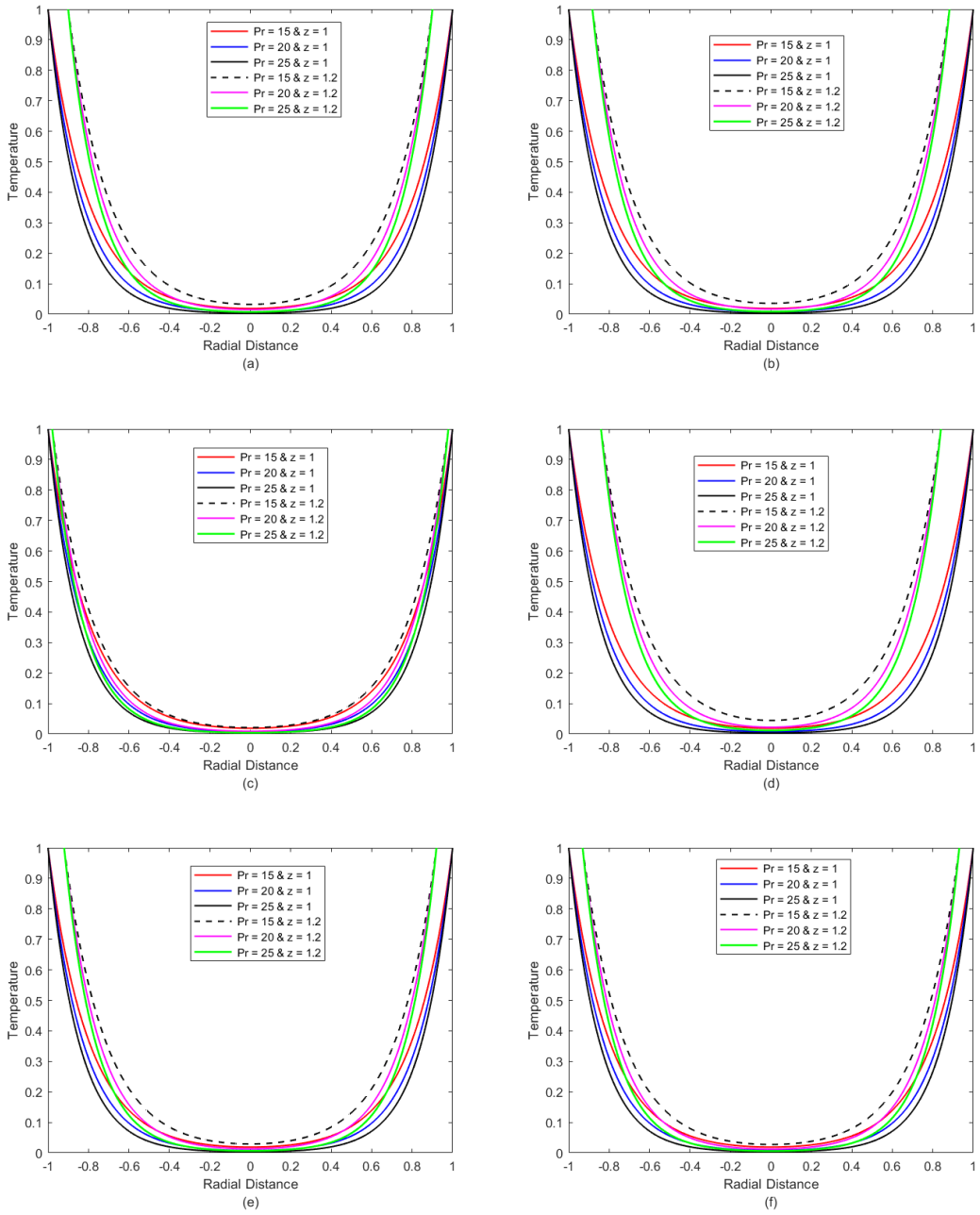

Figure 6 Variations in the temperature profiles of (a) symmetric, (b) elliptical, (c) bell-shaped, (d) trapezoidal, (e) triangular and (f) cosine shapes stenosis artery with $Pr = 15,\ 20$ and 25 for various locations of stenotic region $z = 1$ and 1.2.

Figures 7 and **8** illustrate the volumetric flow rate profiles for various factors, such as magnetic number, Pressure gradient, darcy number and pulse rate. **Figure 7**(**a**) displays the effect of M on the profile of the volumetric flow rate. When $M = 2, 3$ increases, the Lorentz force opposes the motion, resulting in decreased velocity and volumetric flow rate values for symmetric, bell-shaped, elliptical, trapezoidal, triangular and cosine-shaped flow profiles. **Figure 7**(**b**) depicts the effect of the Pressure gradient on the profile of the volumetric flow rate. When Pressure gradient($P_0 = 7, 10$)values grow then the volumetric flow rate profile for areas that have restricted flow increases. **Figure 8**(**a**) depicts the effect of Darcy number on the profile of the volumetric flow rate. As the Darcy number ($Da = 0.05, 0.09$) rises, the volumetric flow rate profile for various types of stenosis flows increases. **Figure 8**(**b**) indicates the influence of pulse rate on the volumetric flow rate curve. The volumetric flow rate profile for distinct sections of artery vessels increases as the pulse rate($w = 0.3, 0.7$) rises.

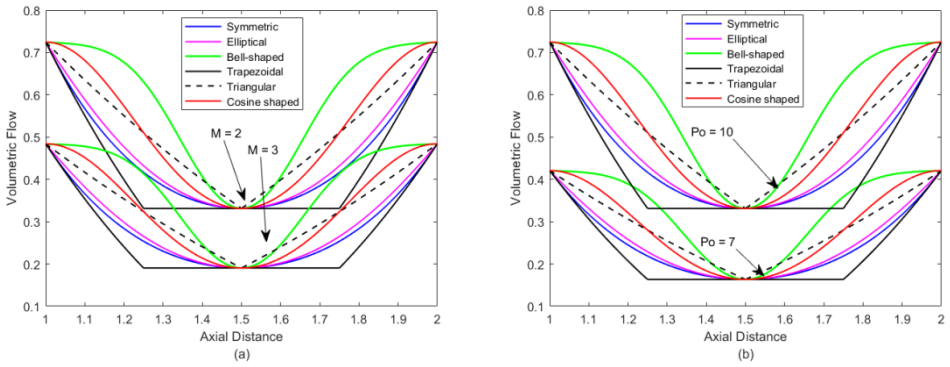

Figure 7 Variations in the volumetric flow rate of symmetric, elliptical, bell-shaped, trapezoidal, triangular and cosine shapes stenosis artery for various value of (a) $M = 2$ and 3 (b) $P_0 = 7$ and $P_0 = 10$.

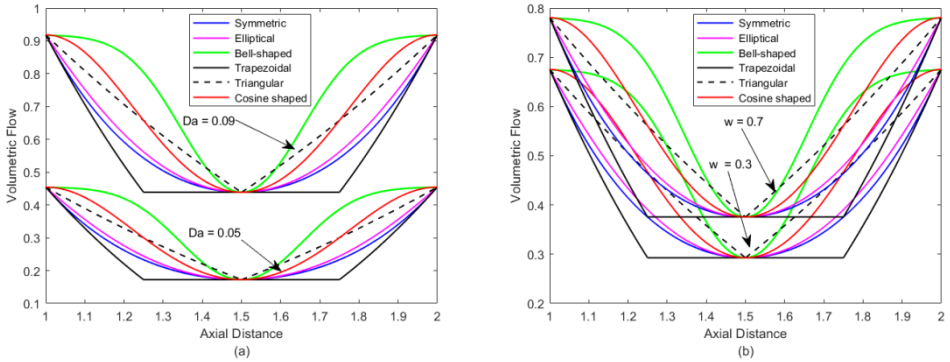

Figure 8 Variations in the volumetric flow rate of symmetric, elliptical, bell-shaped, trapezoidal, triangular and cosine shapes stenosis artery for various value of (a) $Da = 0.05$ and 0.09 (b) $w = 0.3$ and $w = 0.7$.

The wall shear stress profiles for various parameters including Grosh of number, Prandlt number, Darcy number and pulse rate are depicted in **Figures 9** and **10**. **Figure 9**(**a**) depicts the effect of M on the wall shear stress. The wall shear stress profile for symmetric, bell-shaped, elliptical, trapezoidal, triangular and cosine-shaped structures rises as the Grosh of number($Gr = 14, 15$) increases because buoyant force dominates the viscous effect. **Figure 9**(**b**) indicates the effect of the Prandtl number on wall shear stress. As the Prandlt number ($Pr = 19, 21$) increases, the wall shear stress profile for all 6 types of geometries diminishes. **Figure 10**(**a**) illustrates the influence of the Darcy number on wall shear stress. As the Darcy number ($Da = 0.06, 0.07$) increases, the wall shear stress profile for variously shaped geometrical structures increases. **Figure 10**(**b**) depicts the relationship between pulse rate and wall shear stress. For all kinds of stenosis, the wall shear stress profile declines as the pulse rate ($w = 0.3, 0.7$) rises.

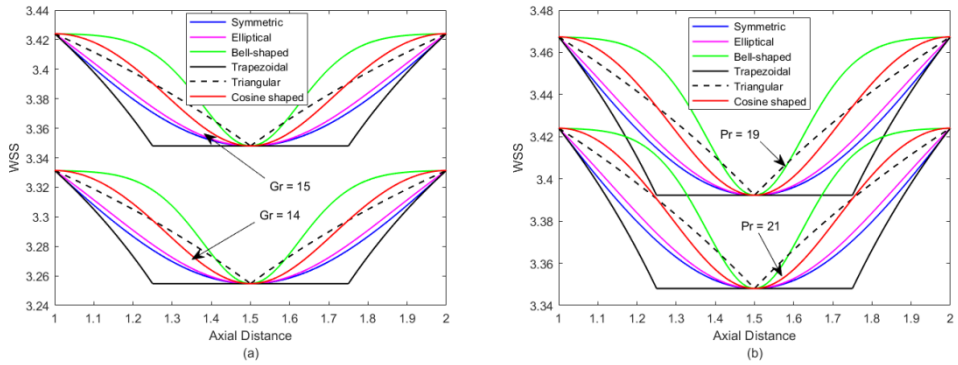

Figure 9 Variations in the wall shear stress of symmetric, elliptical, bell-shaped, trapezoidal, triangular and cosine shapes stenosis artery for various value of (a) $Gr = 14$ and 15 (b) $Pr = 19$ and 21.

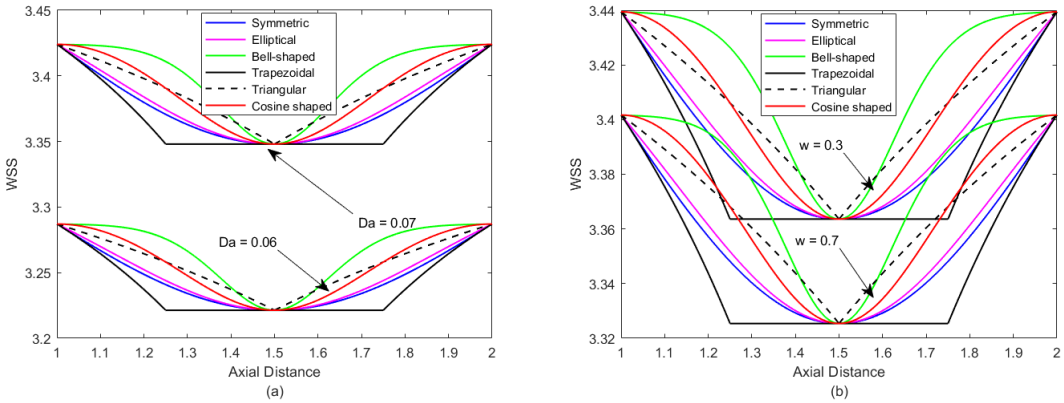

Figure 10 Variations in the wall shear stress of symmetric, elliptical, bell-shaped, trapezoidal, triangular and cosine shapes stenosis artery for various value of (a) $Da = 0.06$ and 0.07 (b) $w = 0.3$ and $w = 0.7$.

Conclusions

This study studied the impact of heat transfer on blood flow through artery walls of different forms between $z = 1$ and $z = 2$. The significant findings of our model include: 1) It has also been discovered that under a magnetic field, blood velocity is greater for bell-shaped artery walls than for trapezoidal artery walls between $z = 1$ and $z = 2$ and all other shapes in between. 2) Under a Darcy number, blood velocity is greater for bell-shaped artery walls between $z = 1$ and $z = 1.2$ than for all other forms, including symmetrical, elliptical, trapezoidal, triangle and cosine-shaped artery walls. 3) If the stenosis is located at $z = 1.2$, the depth of stenosis for all varieties of stenosis, including symmetric, elliptical, bell-shaped, trapezoidal, triangular and cosine-shaped, differs, whereas at $z = 1$, the radial distance is the same in all circumstances. 4) Due to the presence of hemoglobin in RBCs, which contains iron oxide particles and is capable of binding oxygen molecules, the blood is greatly impacted by the magnetic field. 5) Prandtl number is inversely proportional to the rate of heat transfer from the artery wall to the fluid (blood).

The current study takes into account the single-phase model of blood flow in the presence of arterial stenosis. It has the possibility to be expanded to 2- and 3-phase variations. Many new stenosis patterns and parameters can also be included.

References

[1] ID Munir, NA Jaafar and S Shafie. Analysis of unsteady solute dispersion in a blood flow of Herschel-Bulkley through a catheterized stenosed artery. *Mal. J. Fund. Appl. Sci.* 2022; **18**, 430-47.

[2] J Tsetimi and E Mamadu. Numerical study of two dimensional steady incompressible Newtonian laminar flow of blood through constricted artery. *Eur. J. Pure Appl. Math.* 2022; **15**, 314-27.

[3] MAEKot and YA Elmaboud. Unsteady pulsatile fractional Maxwell viscoelastic blood flow with Cattaneo heat flux through a vertical stenosed artery with body acceleration. *J. Therm. Anal. Calorim.* 2021; **147**, 4355-68.
[4] Manisha and S Kumar. Effect of cosine shape stenosis on non-Newtonian blood flow with Casson model in stenosed artery. *Int. J. Eng. Trends Tech.* 2022; **70**, 336-46.
[5] MK Sharma, PR Sharma and V Nasha. Pulsatile blood flow through stenosed artery with axial translation. *Int. J. Biomath.* 2015; **8**, 1550028.
[6] MK Sharma, PR Sharma and V Nasha. Pulsatile MHD arterial blood flow in the presence of double stenoses. *J. Appl. Fluid Mech.* 2013; **6**, 331-8.
[7] MA Kabir, MF Alam and MA Uddin. Numerical simulation of pulsatile blood flow: A study with normal artery, and arteries with single and multiple stenosis. *J. Eng. Appl. Sci.* 2021; **68**, 24.
[8] B Tripathi and BK Sharma. Effect of variable viscosity on MHD inclined arterial blood flow with chemical reaction. *Int. J. Appl. Mech. Eng.* 2018; **23**, 767-85.
[9] KW Bunonyo, C Israel-Cooley and E Amos. Modeling of blood flow through stenosed artery with heat in the presence of magnetic field. *Asian Res. J. Math.* 2018; **8**, 37767.
[10] SNAMZ Abidin, NA Jaafar and Z Ismail. Exact analysis of unsteady convective diffusion in Herschel-Bulkley fluid flow-application to catheterized stenosed artery. *CFD Lett.* 2022; **14**, 75-87.
[11] BK Sharma, R Gandhi and MM Bhatti. Entropy analysis of thermally radiating MHD slip flow of hybrid nanoparticles (Au-Al_2O_3/Blood) through a tapered multi-stenosed artery. *Chem. Phys. Lett.* 2022; **790**, 139348.
[12] M Yadav, S Kumar, A Kaushik, RK Garg, A Ahlawat and D Chhabra. Modeling and simulation of piezo-beam structure mounted in a circular pipe using laminar flow as energy harvester. *Int. J. Eng. Trends Tech*. 2023; **71**, 296-314.
[13] V Kumar, R Kumar, S Gupta, KK Kataria, S Chaudhary and S Dangi. Enhancement of heat transfer performance of a channel flow using modified delta winglet vortex generator. *Adv. Mater. Process. Tech.* 2022, https://doi.org/10.1080/2374068X.2022.2099656
[14] Poonam, BK Sharma, C Kumawat and K Vafai. Computational biomedical simulations of hybrid nanoparticles (Au-Al_2O_3/blood-mediated) transport in a stenosed and aneurysmal curved artery with heat and mass transfer: Hematocrit dependent viscosity approach. *Chem. Phys. Lett.* 2022; **800**, 139666.
[15] R Ponalagusamy and S Priyadharshini. A numerical model on pulsatile flow of magnetic nanoparticles as drug carrier suspended in Herschel-Bulkley fluid through an arterial stenosis under external magnetic field and body force. *Int. J. Comput. Math.* 2019; **96**, 1763-86.
[16] M Chitra and R Bhaskaran. The influence of heat transfer on two phase visco-elastic fluid model for MHD oscilliatory blood flow in stenosed arteries. *Int. J. Inf. Comput. Sci.* 2019; **6**, 31-43.
[17] AK Roy, AK Saha, R Ponalagusamy and S Debnath. Mathematical model on magneto-hydrodynamic dispersion in a porous medium under the influence of bulk chemical reaction. *Korea Aust. Rheol. J.* 2020; **32**, 287-99.
[18] R Manchi and R Ponalagusamy. Modeling of pulsatile EMHD flow of *Au*-blood in an inclined porous tapered atherosclerotic vessel under periodic body acceleration. *Arch. Appl. Mech.* 2021; **91**, 3421-47.
[19] S Mukhopadhyay. Insight into distribution of wall pressure, wall shear stress, and oscillatory shear index: Pulsatile flow of blood subject to Lorentz force. *Force Mech.* 2022; **8**, 100110.
[20] A Hussain, L Sarwar, A Rehman, S Akbar, F Gamaoun, HH Coban, AH Almaliki and MS Alqurashi. Heat transfer analysis and effects of (silver and gold) nanoparticles on blood flow inside arterial stenosis. *Appl. Sci.* 2022; **12**, 1601.
[21] U Khanduri and BK Sharma. *Entropy analysis for MHD flow subject to temperature-dependent viscosity and thermal conductivity*. *In*: S Banerjee and A Saha (Eds.). Nonlinear dynamics and applications. Springer Proceedings in Complexity. Springer, Cham, Switzerland, 2022, p. 457-71.
[22] S Changdar and S De. Analysis of non-linear pulsatile blood flow in artery through a generalized multiple stenosis. *Arab. J. Math.* 2016; **5**, 51-61.
[23] C Kumawat, BK Sharma, QM Al-Mdallal and MRahimi-Gorji. Entropy generation for MHD two phase blood flow through a curved permeable artery having variable viscosity with heat and mass transfer. *Int. Commun. Heat Mass Transf.* 2022; **133**, 105954.
[24] R Ponalagusamy and S Priyadharshini. Couple stress fluid model for pulsatile flow of blood in a porous tapered arterial stenosis under magnetic field and periodic body acceleration. *J. Mech. Med. Biol.* 2017; **17**, 1750109.

[25] R Gandhi, BK Sharma, C Kumawat and OA Beg. Modeling and analysis of magnetic hybrid nanoparticle (Au-Al_2O_3/blood) based drug delivery through a bell-shaped occluded artery with joule heating, viscous dissipation and variable viscosity effects. *J. Process Mech. Eng.* 2022; **236**, 2024-43.

[26] R Gandhi and BK Sharma. *Unsteady MHD hybrid nanoparticle (Au-Al_2O_3/blood) mediated blood flow through a vertical irregular stenosed artery: Drug delivery applications*. *In*: S Banerjee and A Saha (Eds.). Nonlinear dynamics and applications. Springer Proceedings in Complexity. Springer, Cham, Switzerland, 2022, p. 325-37.

[27] KW Bunonyo and L Ebiwareme. A low Prandtl number haemodynamic oscillatory flow through a cylindrical channel using the Power Series Method. *Eur. J. Appl. Phys.* 2022; **4**, 56-65.

[28] S Kumar and S Kumar. Blood flow through an elliptical stenosed artery with the heat source and chemical reaction. *Res. J. Biotechnol.* 2022; **17**, 82-90.

[29] RR Hanvey and KW Bunonyo. Effect of treatment parameter on oscillatory flow of blood through an atherosclerotic artery with heat transfer. *J. Niger. Soc. Phys. Sci.* 2022; **4**, 682.

[30] R Ponalagusamy and R Manchi. A study on two-layered (K.L-Newtonian) model of blood flow in an artery with six types of mild stenoses. *Appl. Math. Comput.* 2020; **367**, 124767.

[31] JKafle, HP Gaire, PR Pokhrel and P Kattel. Analysis of blood flow through curved artery with mild stenosis. *Math. Model. Comput.* 2022; **9**, 217-25.